Atmósfera 40, 95-108 (2026)
https://doi.org/10.20937/ATM.53510

Historical study of the evolution of climate patterns in Puerto Ángel, Oaxaca (1941-1978)

Jorge CASTRO-LÓPEZ*, Laura Fabiola VITAL-MARTÍNEZ, Javier SALINAS-LUNA, Juan MENTADO-MORALES, Ricardo Rodrigo HERNÁNDEZ-HERNÁNDEZ and Miguel Ángel AHUMADA-SEMPOAL

Universidad del Mar, Puerto Ángel, 70902 San Pedro Pochutla, Oaxaca, México.
*Corresponding author; email: sire.jorge@gmail.com

Received: June 26, 2025; Accepted: October 13, 2025

RESUMEN

Este estudio aborda la escasez de datos climatológicos en el suroeste de México mediante la compilación de un registro histórico de temperatura y precipitación en Puerto Ángel, Oaxaca. El análisis utilizó datos *in situ* procesados de la CONAGUA (1941-1978), complementados con datos recientes de satélite de temperatura atmosférica y temperatura superficial del mar (TSM) para cubrir períodos con registros escasos. Metodológicamente, la investigación empleó análisis de componentes principales (PCA) y estadística descriptiva. Se calcularon 16 índices de cambio climático relevantes para regiones tropicales utilizando RClimDex, excluyendo los fenómenos relacionados con las heladas. Las series de tiempo de satélite se descompusieron en tendencia, estacionalidad y residuos mediante el método STD, y los análisis se realizaron principalmente en Octave con el lenguaje M. Los hallazgos clave revelan un aumento de la temperatura durante la década de 1940, que coincide con patrones nacionales y globales. Se identificó una fuerte correlación entre los años de lluvias abundantes y los eventos de El Niño, mientras que los años más fríos coincidieron con La Niña. Los datos satelitales muestran una clara tendencia al calentamiento tanto de la temperatura atmosférica como de la TSM a partir de la década de 2010. Este calentamiento se manifiesta en la desaparición de los récords históricos de bajas temperaturas y en el aumento de las temperaturas máximas en los últimos años. En consecuencia, la región experimenta eventos extremos más frecuentes, lo cual se evidencia por la alta cantidad de huracanes intensos que han tocado tierra en la costa de Oaxaca desde la década de 1990, con una concentración notable a partir de la década de 2010 (p.ej., Frank, Carlotta, Bárbara, Ágata). El estudio concluye que la costa de Oaxaca es altamente sensible a las anomalías climáticas globales y regionales.

ABSTRACT

This study addresses the climatological data gap in southwestern Mexico by compiling a historical record of temperature and precipitation in Puerto Ángel, Oaxaca. The analysis used processed in situ data from CONAGUA (1941-1978), supplemented with recent satellite-derived atmospheric and sea surface temperature (SST) data to cover periods with sparse records. Methodologically, the research employed principal component analysis (PCA) and descriptive statistics. Sixteen relevant climate change indices for tropical regions were calculated using RClimDex, excluding frost-related phenomena. The satellite time series were decomposed into trend, seasonality, and residuals using the STD method, with analyses primarily conducted in Octave using the M language. Key findings reveal a temperature increase during the 1940s, aligning with national and global patterns. A strong correlation was identified between abundant rainfall and El Niño events, while the coldest years coincided with La Niña. Satellite data show a clear warming trend in both atmospheric temperature and SST from the 2010s onward. This warming is evidenced by the disappearance of historical cold records and an increase in recent maximum temperatures. Consequently, the region experiences more frequent extreme events, evidenced by a high number of intense hurricanes making landfall on the Oaxacan coast since the 1990s, with a notable concentration from the 2010s (e.g., Frank, Carlotta, Barbara, Agatha). The study concludes that the Oaxacan coast is highly sensitive to global and regional climate anomalies.

Keywords: climate change indices, principal component analysis, STD time series decomposition, Oaxacan coast.

1. Introduction

Global warming has been documented since the last century and is primarily attributed to the greenhouse effect (Thota, 2025). Similarly, global climate change, driven by rising atmospheric temperatures, has been extensively recorded and studied since the 1970s (Hansen et al., 1988). However, regional studies examining these effects remain scarce along the Oaxacan coast. This paper seeks to establish a foundational climatological precedent for the region by analyzing data from two meteorological stations of the Comisión Nacional del Agua (National Water Commission, Conagua) located in Puerto Ángel, with a focus on the period from 1941 to 1978 (Conagua, 2023).

Among the key findings, a significant increase in global atmospheric temperature was observed during the 1940s. This decade also witnessed two strong El Niño events (1939-1941 and 1946-1947). Notably, the town of Puerto Ángel recorded a corresponding rise in atmospheric temperature, along with anomalous rainfall patterns associated with these El Niño episodes. These results underscore the sensitivity of the Oaxacan coast to climate variability and highlight the importance of localized studies of key climatic variables.

The Intergovernmental Panel on Climate Change (IPCC, 2007, 2012) has warned that climate change is already evident due to global warming. Rising temperatures trigger further climatic phenomena, including polar ice melt, sea-level rise, increased frequency of extreme events such as El Niño, and ocean warming (Trenberth and Smith, 2005). Figure 1 illustrates the steady increase in global mean temperature over time.

In Mexico, a rise in atmospheric temperature has also been documented (Estrada, 2020). Through the Estudio México program (1994-1996), the National Autonomous University of Mexico (UNAM) concluded that Mexico is highly vulnerable to climate change.

This vulnerability has become evident in recent years (Estrada et al., 2023). For instance, one of the most severe droughts on record affected over 1230 municipalities (more than half of the country) keeping them under severe drought conditions from July 15, 2023 to June 30, 2024. As a result, 1.7 million ha of land yielded no harvest, representing a 12.8%

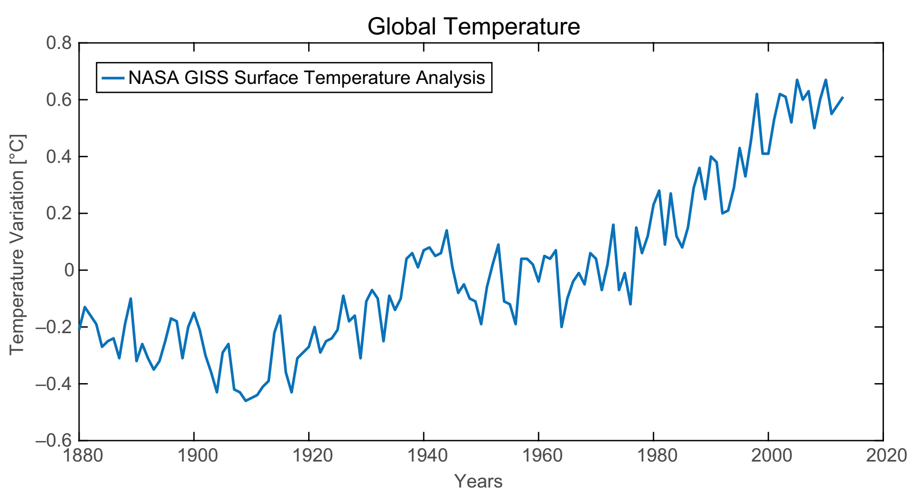

Fig. 1. Global evolution of average annual air temperature.

decrease compared to the previous year (Le Clercq-Ortega et al., 2024). In addition to monitoring atmospheric temperature, new statistical techniques based on daily extreme values are emerging to detect climate change. The IPCC has endorsed a set of 40 indices derived from such methods.

This study computes 16 of these indices to visualize trends in climate variables and analyzes the resulting patterns. Principal component analysis (PCA) is applied to identify rainfall patterns within the recorded time series. To broaden the perspective, sea surface temperature data from NOAA (1981-2023) are decomposed—using the seasonal-trend decomposition (STD) method and implemented in the M language via the Octave compiler—into seasonal, trend, and residual components. The same decomposition is applied to atmospheric temperature data from NASA for Puerto Ángel over the same period.

The analysis reveals an upward trend in both temperature series, consistent with and complementary to earlier findings.

2. Methodology

This study involves collecting atmospheric temperature and precipitation data from the two sole meteorological stations in Puerto Ángel, Oaxaca. The dataset undergoes quality control, including gap-filling between the two series via linear interpolation and the use of values from previous cycles under comparable conditions. The processed data are then used to compute 16 of the 27 climate change indices defined by the Expert Team on Climate Change Detection and Indices (ETCCDI), and PCA is applied to identify rainfall patterns.

Furthermore, satellite-derived time series for atmospheric temperature from NASA and sea surface temperature (SST) from NOAA are obtained for Puerto Ángel, covering the period from 1981 to 2023. These series are decomposed into their seasonal, residual, and trend components to elucidate underlying patterns and long-term behavior.

- This study characterizes the climatology of Puerto Ángel, Oaxaca, across multiple time periods.
- Sixteen of the 27 climate change indices established by the ETCCDI are qualitatively assessed. Indices related to near-freezing temperatures (e.g., snowfall frequency) are excluded due to their irrelevance in this tropical region.
- Daily rainfall data are employed to identify precipitation patterns through principal component analysis (PCA).
- Using remotely sensed data from NOAA (2023) and NASA (2024), SST and atmospheric temperature time series are decomposed into seasonal, trend, and residual components to analyze their temporal behavior and long-term changes.

Puerto Ángel is a bay situated on the Pacific coast of the state of Oaxaca, Mexico, at 15º 40’ 0” N and 96º 29’ 26” W. According to naval meteorological records (Semar, 2024), the region has a warm climate, with a mean annual temperature of 33 ºC and a relative humidity of 66%. The rainy and hurricane season extends from May to November.

- Human settlements in Puerto Ángel date back to pre-Hispanic times, when the bay served as a safe harbor for trade along the Pacific coast.
- The climate is classified as sub-humid with summer rainfall. As a cyclogenetic zone (Castro-Lopez, 2020), the region experiences tropical storms and has a historical record of hurricane impacts. The mean annual temperature exceeds 26 ºC.
- The coastal dynamics are influenced by the Mexican Coastal Current (MCC). Wave activity is particularly pronounced during the swell season (April to May). Seasonal upwellings occur in winter, and freshwater is discharged through the Aguaje stream during the rainy season.
- The area exhibits high biodiversity, including terrestrial species such as iguanas and various snakes, a wide diversity of birds, and marine life such as turtles, corals, and mollusks.

The meteorological stations from which the data were obtained are Conagua 20092 and Conagua C20194 (both in Puerto Ángel, municipality of San Pedro Pochutla, state of Oaxaca).

Finally, the atmospheric temperature time series was obtained from NASA, covering the period from 1981 to 2022. The data were retrieved at the same geographic coordinates (latitude and longitude) as those of meteorological station C20194. SST data were sourced from the Coral Reef Watch SST database (v. 3.1, 1985-present), available through the NOAA, specifically for the location at 15.65º N, 96.50º W in Puerto Ángel Bay.

The STD method by Dudek (2023) was applied to both time series to isolate their seasonal, trend, and residual components. This method uses cycle averaging to extract seasonality and interval averaging to identify long-term trends, while also accounting for irregularities (noise) in the data.

3. Data quality control

Homogeneity in atmospheric data seeks to remove data that comes from non-climatic events such as failures in data capture, technical failures in collection devices, etc., which produce inconsistencies such as the lack of data itself, abrupt jumps or anomalous peaks, duplicate days, daily minimum temperatures higher than the maximum temperatures of that day, etc. This is done through statistical methods. In particular, RHTest v. 4 uses decision-making algorithms such as C4.5 (Salzberg, 1994), which mainly consists of the following:

- **Change point detection.** The core of the method is the penalized maximum F test (PMFT), which operates as follows:
  - Identification of breakpoints: the algorithm systematically scans each point in the time series to determine if a statistically significant change (an inhomogeneity) occurred.
  - Penalty factor: A key feature of the test is the incorporation of a penalty factor (e.g., the Schwarz criterion). This is crucial for preventing the overestimation of change points, thereby avoiding the detection of false jumps that are merely part of the system's natural variability.

- **Adjustment of inhomogeneities.** Once change points are identified, the program adjusts the series to achieve homogeneity using a piecewise regression analysis:
  - Segmentation: the time series is divided into segments at each detected change point. For instance, a change point identified in 1995 would result in two segments: 1941-1995 and 1996-2020.
  - Base segment adjustment: the entire series is adjusted to align with a base segment—typically the most recent or most reliable segment (e.g., 2000-2020). This is done by adding or subtracting the necessary offset to the preceding segments (e.g., 1941-1999) so that the mean over the entire period becomes consistent with the base segment.

Homogeneity processes provide a more reliable database by having smooth fluctuations, thus achieving a representative series of atmospheric processes.

- **Gap filling.** Gap filling was performed using the following methods:
  - Seasonal interpolation based on cyclical trends.
  - Interpolation using seasonal mean or median values.

These procedures were implemented in the M programming language through the Octave compiler, utilizing the statistics package for computational support.

- **Calculation of the trend.** The primary method used by RClimDex is Sen's Slope Estimator, combined with the Mann-Kendall test to assess statistical significance. Trends in climate change indices were calculated using the Sen's slope estimator, and their statistical significance was assessed using the Mann-Kendall test. These nonparametric methods are recommended for analyzing climate series due to their robustness to non-normality and extreme values.

3.1 Inhomogeneities

Inhomogeneities, which can be sudden jumps or steps in the data series, are shown in the first series below, which covers the period from 1941 to 1978 and corresponds to the time series of daily maximum temperature (Fig. 2).

RHtests correct and detect inhomogeneities, and these corrected data are used to analyze the graphs and calculate climate change indices.

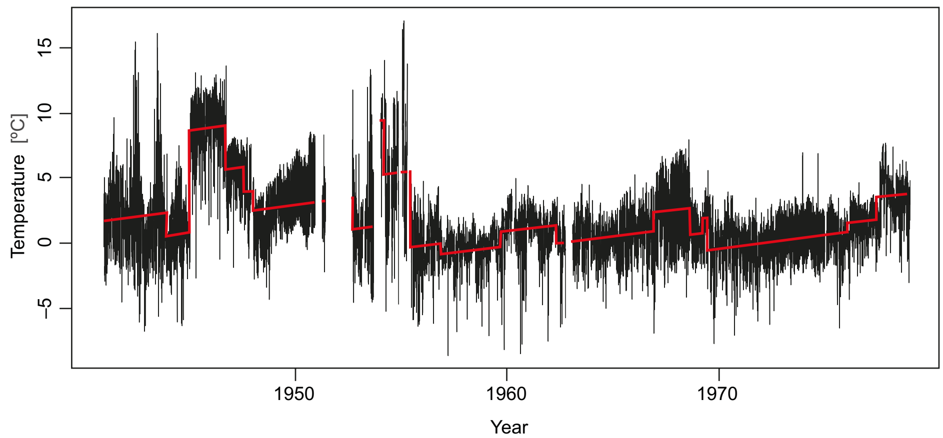

Fig. 2. Data inhomogeneity in daily maximum temperatures from 1941 to 1978.

4. Review of the results

4.1 Station C20194

Before analyzing the graphs with the data already processed with RHtests, let's remember that in Mexico, the effects of El Niño and La Niña (opposite phases of the ENSO phenomenon, the El Niño-Southern Oscillation) are manifested mainly in changes in precipitation patterns, temperature, and hurricane frequency (Chakravorty et al., 2020). El Niño is the warm phase and is characterized by droughts in the north and rains in the south, with increased hurricane formation in the Pacific; La Niña is the cold phase and is characterized by hurricanes in the Gulf of Mexico and colder winters (Boncheva and Kachok, 2019).

Table I shows the monthly average precipitation during the period 1941-1978 and the monthly average temperature, as well as the total precipitation and average temperature throughout that period.

The average temperature reported by different sources (the National Meteorological Service [SMN] of Mexico, NASA Power, Weatherbase, or Climate-Data [2023]) is in the range of 25 to 28 ºC with variations typical of the seasons of the year, that is:

- Warm season (March-May) with maximum temperatures of 30 to 32 ºC.
- Rainy season (June-October) with temperatures between 26 and 28 ºC.

Table I. Average and mean monthly precipitation and temperature.

Months	Average monthly precipitation (mm)	Average monthly temperature $(t_{max} + t_{min})/2$ (ºC)	Average temperature (ºC)	Total precipitation (mm)
January	6.15	27.344	28.03	751.87
February	0.5	27.00		
March	1.71	28.131		
April	0.86	29.221		
May	31.81	30.025		
June	156.61	29.474		
July	113.63	28.462		
August	139.08	28.438		
September	207.17	27.932		
October	69.65	28.27		
November	18.90	28.03		
December	5.75	27.121		

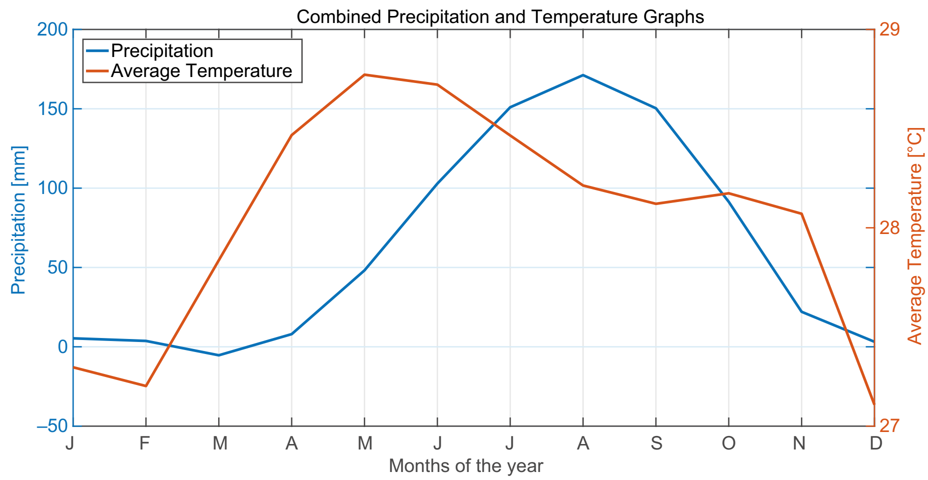

Fig. 3. Combined curves of precipitation and average monthly temperature during the period 1941-1978.

- Cool season (November-February) with minimum temperatures of 20 to 22 ºC.

Figure 3 shows the combined curves of precipitation and atmospheric temperature. When the temperature curve lies above the precipitation curve, the dry season occurs; conversely, when the temperature curve lies below the precipitation curve, the rainy season occurs.

Analyzing Figure 3 and performing a principal component analysis, Table II, help us determine the rainy and dry seasons in the region during the aforementioned period.

Table II. Rainy and dry seasons.

Months	Factor 1	Factor 2
January	0.7729	0.3474
February	0.8402	0.2852
March	0.8267	0.2554
April	0.8349	0.2719
May	0.2603	–0.0943
June	–1.3701	–2.1493
July	–0.6253	–0.5252
August	–0.6758	–0.4370
September	–2.1235	2.2719
October	–0.1419	–0.5622
November	0.6251	0.0483
December	0.7764	0.2881

4.2 Station C20092

4.2.1 1982-2001

The period 1982-2001 falls between two intervals with no data collection (1978-1981 and 2001-2015).

Table III shows the monthly average precipitation, the monthly average temperature, and the total precipitation throughout that period. Meanwhile, Figure 4 shows the combined curves of precipitation and atmospheric temperature, indicating that when the temperature curve lies above the precipitation curve, it is the dry season; conversely, when the temperature curve lies below the precipitation curve, it is the rainy season.

4.3.1 2015-2021

Table IV shows the monthly average precipitation, the monthly average temperature, and the total precipitation throughout that period. In turn, Figure 5 shows the combined curves of precipitation and atmospheric temperature, noting that when the temperature curve is above the precipitation curve, it is the dry season, and conversely, when the temperature curve is below the precipitation curve, it is the rainy season.

5. Climate change indices

The quality and quantity of the data collected from the periods 1982-2001 and 2015-2021 do not allow an adequate calculation of the indices; therefore,

Table III. Average and mean monthly precipitation and temperature.

Months	Average monthly precipitation (mm)	Average monthly temperature $(t_{max} + t_{min})/2$ (ºC)	Average temperature (ºC)	Total precipitation (mm)
January	1.96	26.28	27.44	162.45
February	0.5	26.50		
March	0.36	26.96		
April	1.24	27.66		
May	8.50	28.38		
June	30.70	28.03		
July	28.34	27.78		
August	31.36	28.13		
September	32.22	27.67		
October	20.55	27.83		
November	3.18	27.60		
December	3.48	26.47		

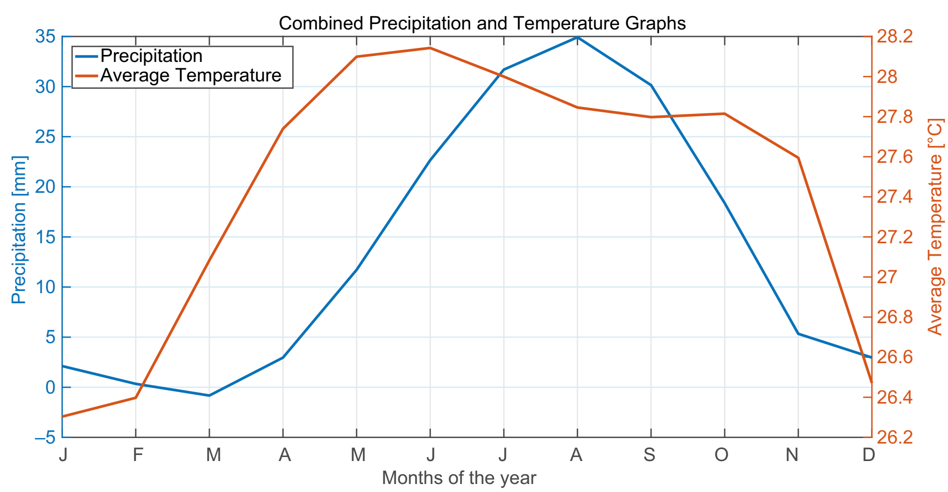

Fig. 4. Combined curves of precipitation and average monthly temperature during the period 1982-2001.

Given Puerto Ángel's geographical position and climatology, not all indices are relevant (e.g., those related to temperatures below 5 ºC), so only indices related to atmospheric temperature and precipitation are chosen.

In the graphs corresponding to the calculation of climate change indices, the empty circles indicate the number of days recorded (or counted, in the case of a number of days) in the corresponding year, indicated on the abscissa. The straight line indicates the trend, and the interval line illustrates the general behavior of the series.

In the time series for the interval 1941-1978, the number of wet days (days with daily precipitation greater than 1mm; RR >= 1mm) decreased from four days in 1941 to three days in 1978, with a maximum of 11 days in 1963, influenced by the El Niño event. Consequently, the trend is a decrease in the number of wet days, with a slope of –0.047, as shown in Figure 6.

For the total number of days per year with precipitation greater than 20 mm, there is also a downward trend with a negative slope of –0.173, which also coincides with the global warming recorded in the

Table IV. Average and mean monthly precipitation and temperature.

Months	Average monthly precipitation (mm)	Average monthly temperature $(t_{max} + t_{min})/2$ (ºC)	Average temperature (ºC)	Total precipitation (mm)
January	4.4	23.32	26.92	1012.6
February	0	23.08		
March	2.88	26.28		
April	0.5	28.48		
May	114.92	29.34		
June	254.08	28.58		
July	103.61	30.31		
August	198.9	28.79		
September	141.46	26.85		
October	164.7	28.68		
November	16.63	24.80		
December	0.52	26.43		

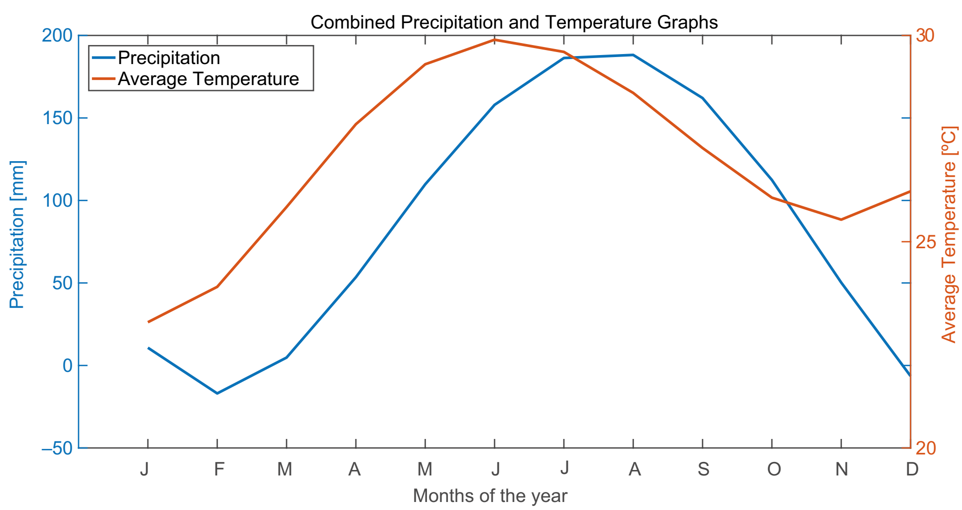

Fig. 5. Combined curves of precipitation and average monthly temperature during the period 2015-2021.

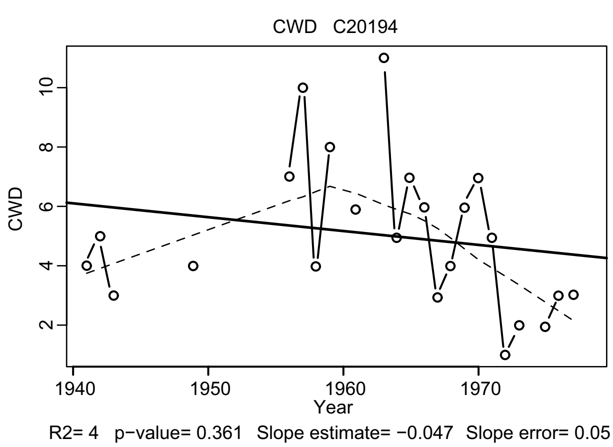

Fig. 6. Number of consecutive days with rainfall greater than 1 mm, RR >= 1 mm (1941-1978). The solid, straight line shows the linear trend, which represents the overall direction of the data. The dotted line shows the weighted trend, which provides or reveals the recent underlying trend.

1940s, since in several years of that decade, there is no record of days with rainfall greater than 20 mm, as can be seen in Figure 7.

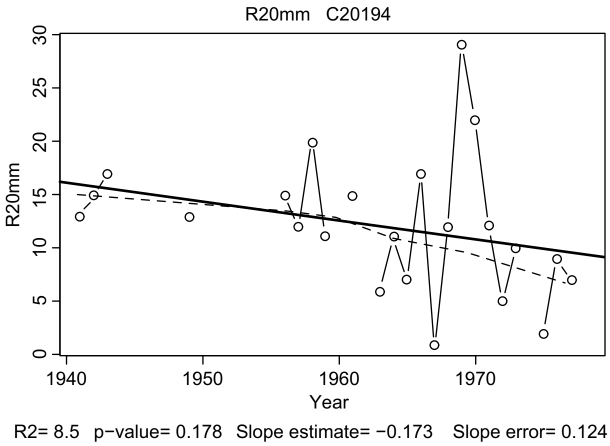

Fig. 7. Number of days with very heavy precipitation (R20mm) (1941-1978). The solid, straight line shows the linear trend, which represents the overall direction of the data. The dotted line shows the weighted trend, which provides or reveals the recent underlying trend.

The average temperature in Puerto Ángel during the three periods shown is 27 ºC. It is higher than that used to estimate the SU25 index, which calculates the number of days with temperature greater than 25 ºC that are summer days or hot in other latitudes, so for Puerto Ángel that does not meet these conditions the summer temperature will be taken as 33 ºC. Thus, from 1941 to 1978, the number of days per year at this temperature decreased, consistent with the period of global warming in the 1940s. The trend is downward with a slope of –0.266. However, the weighted trend falls to a minimum in the late 1950s and begins to rise until 1978, as can be seen in Figure 8.

Consistent with the fact that summer days and nights in Puerto Ángel are warmer than those established in the TR20 indicator (which calculates the number of tropical nights), in this work the highest minimum daily temperature was considered (24.1 ºC). As can be seen in Figure 9, there is a downward trend with a slope of –1.35.

Figure 10 shows days with extreme temperatures, indicating more pronounced global warming in the 1940s, with temperatures reaching up to 48 ºC in 1942 and 1943. Once this period had passed and at-

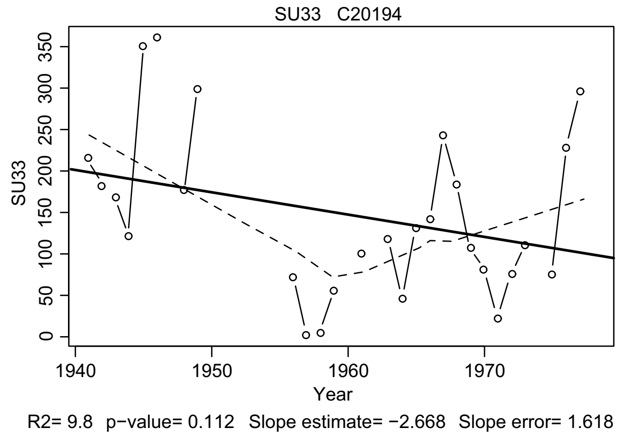

Fig. 8. Summer days. The solid, straight line shows the linear trend, which represents the overall direction of the data. The dotted line shows the weighted trend, which provides or reveals the recent underlying trend.

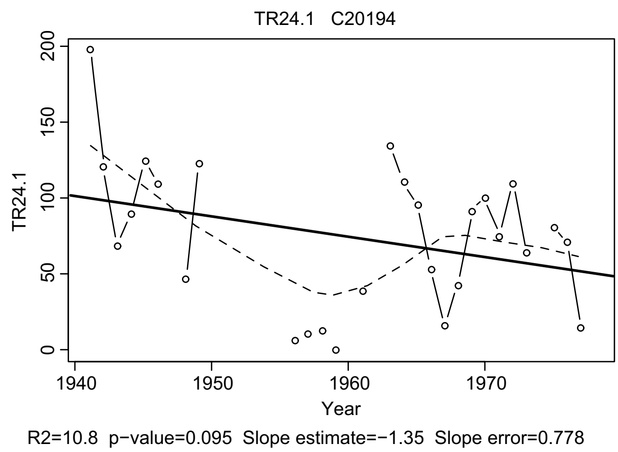

Fig. 9. Tropical nights. The solid, straight line shows the linear trend, which represents the overall direction of the data. The dotted line shows the weighted trend, which provides or reveals the recent underlying trend.

mospheric temperatures had stabilized, the influence of the El Niño event was evident in subsequent years, with temperatures rising to 40 ºC.

The number of consecutive days without rain decreased as the period of global warming ended; that is, during the 1940s, when atmospheric temperatures were higher, it rained more than after that period. Figure 11 shows an upward trend with a slope of 2.66, indicating that the dry season lengthened rapidly.

The average maximum temperature in 1945 was 40 ºC, which indicates the magnitude of global

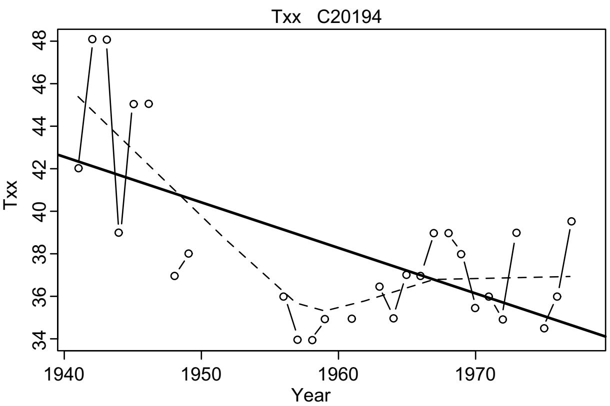

Fig 10. Extreme maximum temperature (Txx). The solid, straight line shows the linear trend, which represents the overall direction of the data. The dotted line shows the weighted trend, which provides or reveals the recent underlying trend.

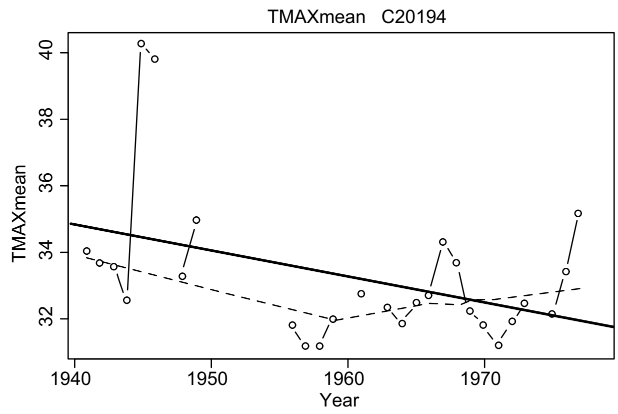

Fig. 12. Average annual maximum temperature (TMAX-mean). The solid, straight line shows the linear trend, which represents the overall direction of the data. The dotted line shows the weighted trend, which provides or reveals the recent underlying trend.

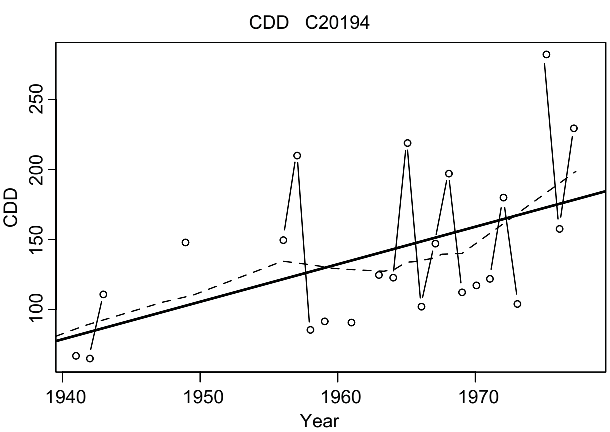

Fig. 11. Consecutive dry days (CDD). The solid, straight line shows the linear trend, which represents the overall direction of the data. The dotted line shows the weighted trend, which provides or reveals the recent underlying trend.

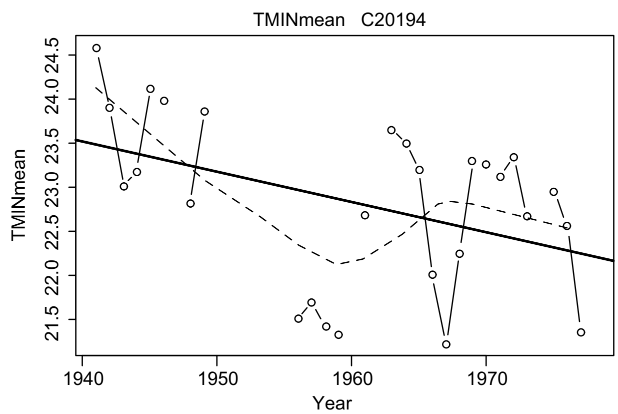

Fig. 13. Average minimum temperature (TMINmean). The solid, straight line shows the linear trend, which represents the overall direction of the data. The dotted line shows the weighted trend, which provides or reveals the recent underlying trend.

warming. This index is decreasing, as indicated by a downward trend with a slope of –0.078 (Fig. 12).

The average minimum temperature also decreases, as shown in Figure 13, where a downward trend with a slope of –0.034 is observed, indicating that minimum temperatures are generally very stable.

Rainfall decreased during this period (1941-1978). As noted above, rainfall was more abundant during a period of global warming than subsequently, including El Niño years. There was a significant peak in 1969 of almost 2000 mm. Figure 14 shows a downward trend with a slope of –10.926.

6. Satellite data

Figure 15 presents the results of applying the seasonal-trend decomposition (STD) method to the atmospheric temperature time series in Puerto Ángel.

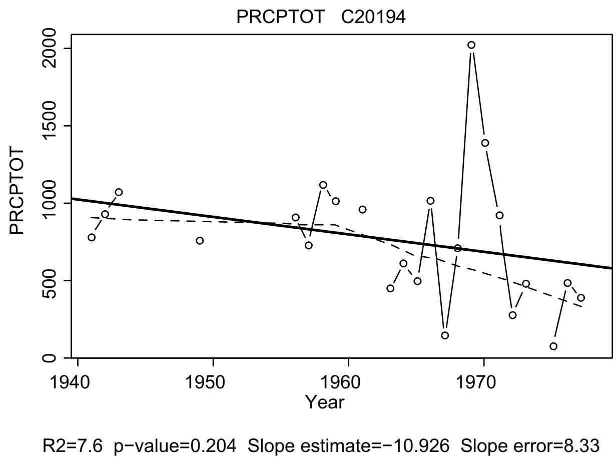

Fig. 14. Total annual precipitation (PRCPTOT). The solid, straight line shows the linear trend, which represents the overall direction of the data. The dotted line shows the weighted trend, which provides or reveals the recent underlying trend.

The first panel displays the original data from 1981 to 2023. The second panel shows the trend component, which reflects the long-term direction of the data and helps identify increasing or decreasing patterns.

The trend reveals fluctuations between 28 and 29 ºC from 1981 to 2014. However, in 2015, a notable maximum of 29.42 ºC was recorded, with a minimum of 29 ºC. From this year onward, trend values increased consistently, remaining within the 29-29.4 ºC range. The previously observed minimum of 28 ºC, common during the 1981-2011 period, was not reached again. By 2023, a new maximum of 29.49 ºC was observed.

These results indicate that since the 2000s, atmospheric temperatures in Puerto Ángel have exhibited higher minimum values compared to earlier decades, confirming a sustained upward trend from the 2000s until 2023. The third panel illustrates the seasonal component, showing a clear cyclical pattern. Finally, the fourth panel presents the residual component, indicating minimal variation around the median.

Figure 16 displays the decomposition of the SST time series into its seasonal, trend, and residual components. The first panel shows the observed SST variations during the study period, while the second panel presents the long-term trend, confirming a gradual increase in SST from 1981 to 2023.

From 1985 to 2012, the SST trend remained within a range of 27.58 to 28.30 ºC, with a minimum recorded in 1988 (27.58 ºC) and a maximum in 1994 (28.30 ºC). This range was exceeded between 2012 and 2016, when values fluctuated from 28.00

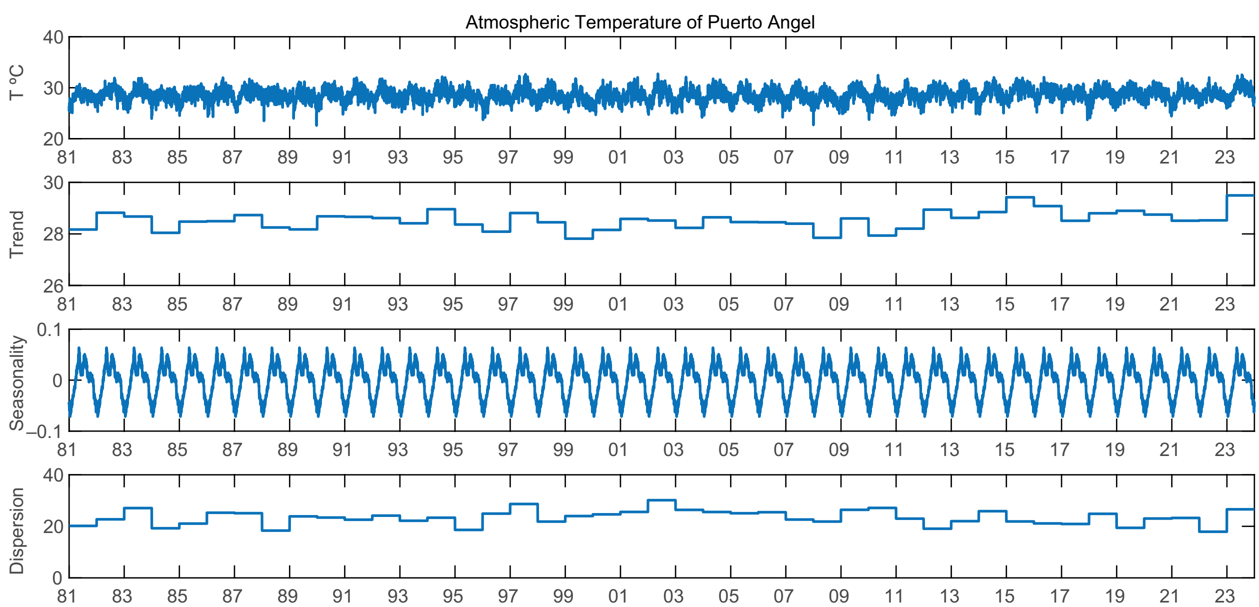

Fig. 15. Results of the STD method for the Puerto Ángel atmospheric temperature variable from 1981 to 2023.

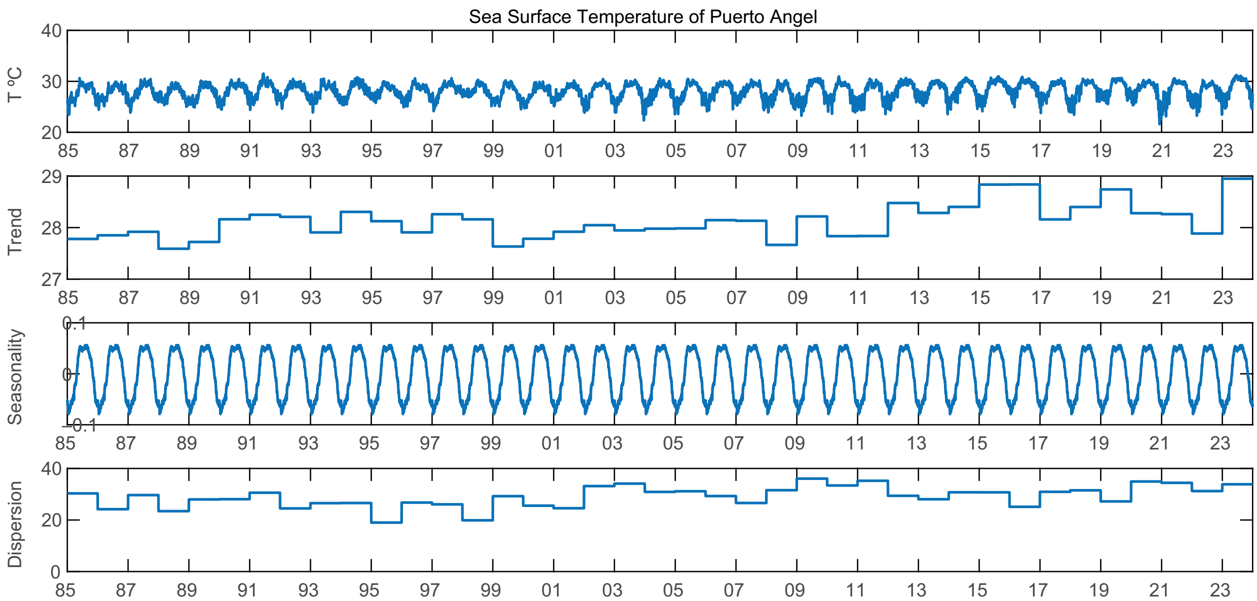

Fig. 16. Results of the trend, seasonality, and dispersion of the sea surface temperature data.

to 28.83 ºC. A slight decrease occurred in 2017 (28.39 ºC), followed by a rebound to 28.74 ºC in 2019. Notably, the trend declined from 2020 to 2022 (reaching 27.88 ºC) but increased considerably in 2023, reaching 28.94 ºC.

The third panel illustrates seasonality, revealing a clear annual cycle with peaks during summer months and troughs in winter, reflecting SST responsiveness to seasonal climate patterns.

7. Conclusions

The results reveal a period of local warming during the 1940s, consistent with a documented global warming phase (Wang, 2023). Climate indices related to atmospheric temperature increase show a general decline after 1950, stabilizing thereafter with peaks occurring primarily during El Niño events. Notably, the number of rainy days was higher even during the warming period, while precipitation became more intense but less frequent afterward—indicating a shift toward fewer but more torrential rainfall events.

Data from station 20092 cover short intervals and include a gap between 2002 and 2014. Moreover, evident inconsistencies are observed in precipitation records for the period 1982-2001. These issues prevent reliable calculation of climate change indices due to insufficient data length and, in the case of rainfall, poor data quality.

Despite the growing importance of the Puerto Escondido-Puerto Ángel-Huatulco corridor in recent decades, no academic program exists to record and analyze the region's climatology. Historically, the federal government maintained only two climatological stations in this entire area, both located in Puerto Ángel. These stations suffer from data gaps, and the absence of additional nearby stations has prevented the construction of a reliable reference series. To address this limitation, descriptive statistics were used to outline the general behavior of atmospheric temperature and precipitation. Additionally, satellite data were used to provide a broad overview of climatic trends during periods with missing records.

Puerto Ángel demonstrates a clear sensitivity to global climate variations. This is evidenced by the historical record of *in situ* data, which shows the warming period of the 1940s and the subsequent return to lower temperatures.

In addition to these global trends, it is crucial to highlight the local effects associated with changes in SST as captured by satellite data. For instance, increased SST during El Niño events leads to torrential rains. It is important to note that the frequency and intensity of this phenomenon have increased, with multi-year events in the last decade that prolong and accumulate the impacts of extreme climates (Li et al., 2024). Conversely, decreased SST resulting from La Niña events causes prolonged droughts, which, as they are also multi-year in nature (Wang, 2023), aggravate their consequences.

These fluctuations—both the historical warming and the El Niño and La Niña cycles—are reflected in the descriptive statistics and the climate change indices analyzed. As shown in the figures, El Niño years are characterized by intense rainfall, while La Niña years are associated with scarce precipitation and slightly lower minimum temperatures.

The economic consequences for the region, and particularly for Puerto Ángel, are considerably severe. The local economy, based on agriculture, fishing, and tourism, is highly vulnerable. This vulnerability is exacerbated by a lack of resilient service infrastructure. A clear example was Hurricane Agatha in 2022, which nearly destroyed the drinking water distribution network and silted up water wells, requiring two years to restore service despite the importance of the tourism sector.

Likewise, rising temperatures and fewer rainy days have forced coffee growers to replace the area's typical shade-grown variety—valued for its complex aroma—with sun-grown coffee, which is lower quality and has a simpler sensory profile, thereby sacrificing product quality.

To address these gaps, atmospheric and SST time series for Puerto Ángel were obtained from satellite data. These series were decomposed into trend, seasonal, and residual components. Seasonality exhibits a clear annual cycle, with maxima during summer months and minima in winter, reflecting the responses of both SST and atmospheric temperature to seasonal climate cycles. Furthermore, the trend in both series has been upward since the early 2010s. New highs and lows have been established, with previous minima no longer observed—a pattern analogous to a sustained "regime shift" in climatic behavior, rarely reversible once established.

This study provides the first historical climatological assessment for Puerto Ángel, Oaxaca, offering a foundation for understanding local climate variability and long-term trends.

Acknowledgments

We extend our gratitude to CONAHCYT and the Universidad del Mar for their support and for providing the opportunity to conduct this research. We also wish to express our sincere thanks to Professor Claudia Mamet for her invaluable assistance with the translation process.

References

Boncheva AI, Kachok R. 2019. Índices de cambio climático en la reserva de la biósfera El Vizcaíno, Baja California Sur, México (1960-2012). Revista Brasileira de Climatologia 24: 67-93. https://doi.org/10.5380/abclima.v24i0.51845

Castro-López J, Zavala-Trujillo B, Figueroa-Lara A. 2020. La física de los huracanes Paulina y Patricia en su paso por el Pacífico mexicano. Revista Mexicana de Física E 17: 33-40. https://doi.org/10.31349/RevMexFisE.17.33

Chakravorty S, Pérez RC, Anderson BT, Giese BS, Larson SM, Pivotti V. 2020. Testing the trade wind charging mechanism and its influence on ENSO variability. Journal of Climate 33: 7391-7411. https://doi.org/10.1175/JCLI-D-19-0727.1

Climate-Data. 2023. Climate data for cities worldwide. Available at: https://en.climate-data.org/ (accessed on October 25, 2023).

Dudek G. 2023. STD: A seasonal-trend-dispersion decomposition of time series. IEEE Transactions on Knowledge and Data Engineering 35: 10339-10350. https://doi.org/10.1109/TKDE.2023.3268125

Conagua. 2023. Servicio Meteorológico Nacional. Available at: https://smn.conagua.gob.mx/es/ (accessed on November, 2023).

Estrada F, Velasco JA, Martínez-Arroyo A, Calderón-Bustamante O. 2020. An analysis of current sustainability of Mexican cities and their exposure to climate change. Frontiers in Environmental Science 8: 25. https://doi.org/10.3389/fenvs.2020.00025

Estrada F, Mendoza A, Murray G, Calderón-Bustamante O, Botzen W, de León-Escobedo T, Velasco JA. 2023. Model emulators for the assessment of regional impacts and risks of climate change: A case study of rainfed maize production in Mexico. Frontiers in Environmental Science 11: 1027545. https://doi.org/10.3389/fenvs.2023.1027545

Hansen J, Fung I, Lacis A, Rind D, Lebedeff S, Ruedy R, Russell G, Stone P. 1988. Global climate changes as forecast by Goddard Institute for Space Studies three-dimensional model. Journal of Geophysical Research Atmospheres 93: 9341-9364. https://doi.org/10.1029/JD093iD08p09341

PCC. 2007. Climate change 2007. Synthesis report. Contribution of Working Groups I, II and III to the Fourth Assessment Report of the Intergovernmental Panel on Climate Change (Pachauri RK, Reisinger A (Eds.). IPCC, Geneva, Switzerland, 104 pp.

IPCC. 2012. Managing the risks of extreme events and disasters to advance climate change adaptation. A special report of working groups I and II of the Intergovernmental Panel on Climate Change (Field CB, Barros V, Stocker TF, Qin D, Dokken DJ, Ebi KL, Mastrandrea MD, Mach KJ, Plattner G-K, Allen SK, Tignor M, Midgley PM, Eds.). Cambridge University Press, Cambridge, UK, and New York, NY, USA, 582 pp.

Le Clercq-Ortega JA, Conde-Álvarez C, Delgado-Ramos GC, Lucatello S. 2024. Principios y mecanismos de justicia climática: derechos ambientales, justicia procesal y litigio climático en México. Recomendaciones de política pública de la REDCIC 2. Red Mexicana de Científicos(as) por el Clima.

Li X, Hu S, Hu Y, Cai W, Jin Y, Lu Z, Guo J, Lan J, Lin Q, Yuan S, Zhang J, Wei Q, Liu Y, Yang J, Nie J. 2024. Persistently active El Niño-Southern Oscillation since the Mesozoic. Proceedings of the National Academy of Sciences 121: e240475812 https://doi.org/10.1073/pnas.2404758121

NASA. 2024. NASA Power. National Aeronautics and Space Administration. Available at: https://power.larc.nasa.gov/ (accessed on February 12, 2024).

NOAA. 2023. CoastWatch data portal. National and Atmospheric Administration. Available at: https://coastwatch.noaa.gov/cw_html/cwViewer.html (accessed on October 15, 2023).

Semar. 2024. Puerto Angel, Oaxaca. Secretaría de Marina. Available at: https://digaohm.semar.gob.mx/cuestionarios/cnarioPtoangel.pdf (accessed on January 9, 2024).

Thota V. 2025. The role of human activity in climate change. Open Access Journal of Multidisciplinary Research 1: 1-17. https://doi.org/10.47760/oajmr.2025.v01i02.001

Trenberth KE, Smith, L. 2005. The mass of the atmosphere: A constraint on global analyses. Journal of Climate 18: 864-875. https://doi.org/10.1175/JCLI-3299.1

Wang L, Wang L, Li Y, Wang J. 2023. A century-long analysis of global warming and earth temperature using a random walk with drift approach. Decision Analytics Journal 7: 100237. https://doi.org/10.1016/j.dajour.2023.100237